JCI The Journal of Clinical Investigation

Emerging lymphatic imaging technologies for mouse and man

Eva M. Sevick-Muraca, … , Sunkuk Kwon, John C. Rasmussen

J Clin Invest. 2014;124(3):905-914. https://doi.org/10.1172/JCI71612.

Review Series

The lymphatic circulatory system has diverse functions in lipid absorption, fluid homeostasis, and immune surveillance and responds dynamically when presented with infection, inflammation, altered hemodynamics, and cancer. Visualization of these dynamic processes in human disease and animal models of disease is key to understanding the contributory role of the lymphatic circulatory system in disease and to devising effective therapeutic strategies. Longitudinal, non-destructive, and repeated imaging is necessary to expand our understanding of disease progression and regression in basic science and clinical investigations. Herein we summarize recent advances in in vivo lymphatic imaging employing magnetic resonance, computed tomography, lymphoscintigraphy, and emerging optical techniques with respect to their contributory roles in both basic science and clinical research investigations.

Emerging lymphatic imaging technologies for mouse and man

Eva M. Sevick-Muraca, Sunkuk Kwon, and John C. Rasmussen

The Center for Molecular Imaging, Brown Foundation Institute of Molecular Medicine, University of Texas Health Science Center, Houston, Texas, USA.

The lymphatic circulatory system has diverse functions in lipid absorption, fluid homeostasis, and immune surveillance and responds dynamically when presented with infection, inflammation, altered hemodynamics, and cancer. Visualization of these dynamic processes in human disease and animal models of disease is key to understanding the contributory role of the lymphatic circulatory system in disease and to devising effective therapeutic strategies. Longitudinal, non-destructive, and repeated imaging is necessary to expand our understanding of disease progression and regression in basic science and clinical investigations. Herein we summarize recent advances in in vivo lymphatic imaging employing magnetic resonance, computed tomography, lymphoscintigraphy, and emerging optical techniques with respect to their contributory roles in both basic science and clinical research investigations.

Introduction

Despite the diverse and dynamic roles that the lymphatic vasculature plays in healthy and pathological processes, there have historically been few methods to non-invasively image the response of lymphatics within in vivo animal models of human disease and even fewer methods suitable for clinical investigations. The interrogation of lymphatics in mice often requires visualization of blue dye–stained lymphatic vessels in dissected tissues or tissue sectioning for immunohistological staining of the lymphatic markers VEGFR-3, prospero-related homeobox 1 (PROX1), podoplanin, and lymphatic vessel endothelial hyaluronan receptor 1 (LYVE1) in order to identify evidence of lymphangiogenesis, lymphatic vessel regression, or changes in function from single snapshots. This is in contrast to the blood vascular circulatory system, which is not only readily visualized in exposed tissues, but is routinely and non-invasively imaged using magnetic resonance (MR) and CT angiographic techniques that involve intravenous delivery of contrast agents. Unfortunately, locating and cannulating a lymphatic vessel can be significantly invasive for clinical research and nearly impossible in basic science investigations that utilize transgenic mouse models. While Doppler ultrasound for functional blood flow imaging depends upon scattering of moving red blood cells, the comparatively acellular lymph escapes interrogation using this technique. Molecular imaging approaches are under development for the diagnosis, stratification, selection, and assessment of molecular therapies in a variety of cardiovascular conditions, including apoptosis, tumor angiogenesis, thrombosis, atherosclerosis, and myocardial infarction (1). However, molecular targets of lymphangiogenesis and lymphatic vessel remodeling have not yet been fully developed, thereby limiting these technologies for basic science and clinical investigations.

The objective of this Review is to first summarize current and emerging in vivo imaging approaches that facilitate both basic science and clinical investigations of lymphatic vasculature, and secondly, to review how these imaging tools can contribute to our understanding of the role of the lymphatic circulation in health and disease first in animal models and then in humans. While there are several reviews on methods for preclinical or clinical lymphatic imaging (2–6), including LN mapping (LNM) (6, 7), herein we emphasize emerging optical imaging and fluorescent protein gene reporter technologies with sufficient in vivo temporal and spatial resolution to provide informative contributions in basic science and/or clinical research investigations of diseases in which the lymphatics are implicated.

Imaging lymphatic architecture in humans and mice

With the exception of clinical MRI of dilated lymphatics with stagnated lymph flow (8) and gene reporter imaging in transgenic animal studies (described below), all current and emerging non-invasive lymphatic imaging approaches require the administration of an exogenous contrast agent (Figure 1). High-resolution lymphangiography of the peripheral and truncal lymphatics requires the administration of exogenous x-ray or MR contrast agents either directly into the lymphatics via cannulation of a lymphatic vessel (direct lymphangiography; Figure 1, route ii) (9) or indirectly into the lymphatic plexus via intradermal injection (indirect or interstitial lymphangiography; Figure 1, route i) (10). Owing to the difficulties of cannulating small lymphatics in mouse models, direct lymphangiography is not employed in basic science investigations. Instead, indirect MR lymphangiography is used, in which gadolinium-based contrast media is injected into the intradermal and subcutaneous spaces that drain into the dermal capillary plexus. The lymphatic capillary plexus within these spaces contains initial lymphatics that have a discontinuous basement membrane and, under normal circumstances, actively take up particle- or fluid-based contrast agents for transport to peripheral and truncal lymphatics before emptying into the blood circulation. Because of the confined space of the capillary plexus, contrast volumes are limited to microliters in animals and to approximately 0.1 ml in humans, although larger volumes of 1 to 5 ml have been injected into the subcutaneous space for slower uptake into the lymphatics. Indirect MR lymphangiography in the legs of lymphedema patients (11–13) has excellent resolution and better visualization than lymphoscintigraphy (14) (Figure 2, A and B), but this technique has not been used for non-invasive imaging of truncal lymphatics, as has been demonstrated with x-ray direct lymphan-

Conflict of interest: Eva M. Sevick-Muraca has received sponsored research funding from Kimberly-Clark Inc. and Tactile Systems Inc. in fields of study that use near-infrared fluorescence imaging and imaging lymphatic function in humans. In addition, Eva M. Sevick-Muraca has financial interests in a university start-up company that seeks to commercialize near-infrared lymphatic imaging.

Citation for this article: *J Clin Invest.* 2014;124(3):905–914. doi:10.1172/JCI71612.

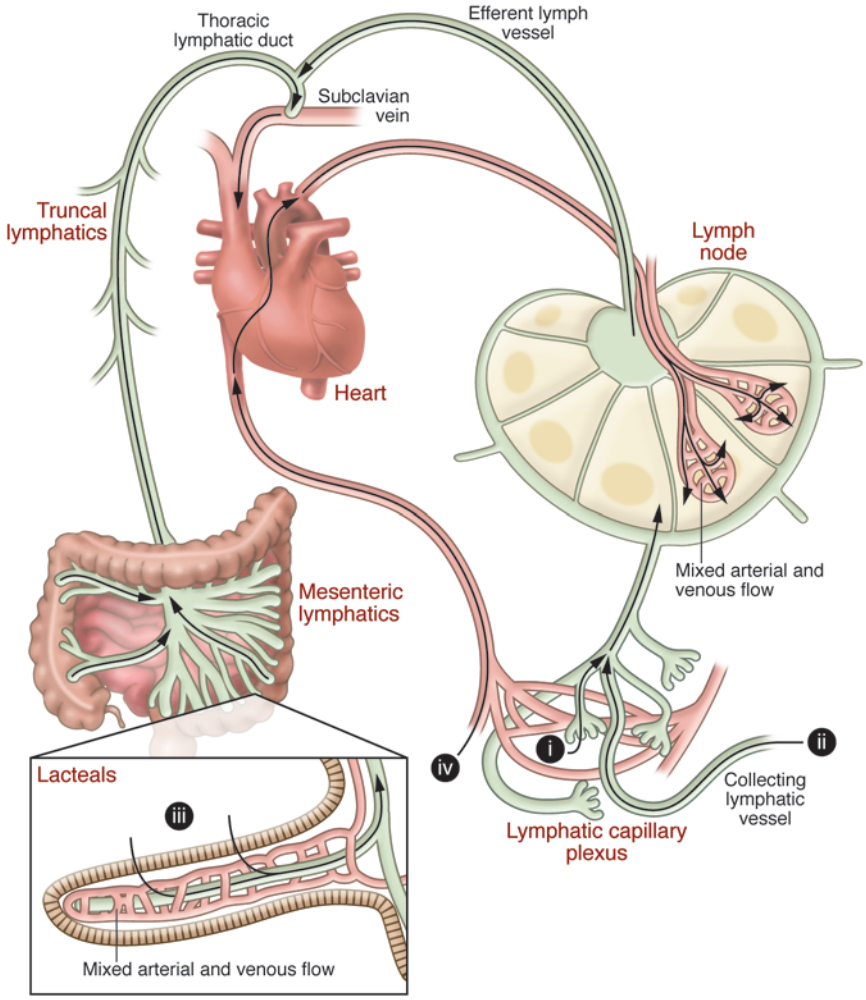

Figure 1
Routes of contrast agent administration. (i) Intradermal/interstitial administration or indirect lymphography results in contrast agent uptake (arrows) into the lymphatic capillary plexus, which is the entry point for the peripheral lymphatics, through collecting and conducting lymphatic vessels, into LNs and eventually into the truncal lymphatics and thoracic duct that drains into the subclavian vein. (ii) Intra-lymphatic administration or direct lymphography consists of cannulating a collecting lymphatic vessel for direct access to the lymphatic vasculature for imaging of peripheral and truncal lymphatics. (iii) Oral gavage of hydrophobic lipids results in uptake through the lacteals into the mesenteric lymphatics that eventually drain to the truncal lymphatics and into the thoracic duct. (iv) Intravenous administration of lymphatic contrast gains access to the lymphatic space predominantly through the high endothelial venules in the LNs or through the reticulo-endothelial system. With the exception of intra-lymphatic administration (ii), these routes of administration are accessible in mouse models of lymphatic disorders.

giography. With advances in MR contrast agent development, indirect MR lymphangiography has enabled the localization of LNs and peripheral lymph drainage pathways in animals (15–18). Albumin-binding gadolinium-based agent gadofosevet, recently FDA-approved for use in hemovascular applications, might also potentially be employed off-label for interstitial, indirect MR lymphangiography (14).

Lymphoscintigraphy (reviewed in refs. 19–21) provides a routine clinical means to assess lymphatic function and architecture in humans, albeit with low spatial and temporal resolution, and is not typically used in investigations employing mouse models of human disease. The technique involves the intradermal administration of a radiocolloid that is taken up by the lymphatics and, typically after hours, imaged using a gamma camera for tens of minutes in order to obtain a grainy image of the lymphatics (see Figure 2B). Lymphatic function can be assessed either by measuring the time between the injection in distant digits and the appearance of tracer in major lymphatic basins, such as the inguinal or axillary LN basins (22), or by monitoring the depot clearance of an intradermally injected agent (23).

Fluorescence microlymphangiography (FML) represents the first fluorescence technique used to non-invasively interrogate the lymphatics in mice or in humans with high resolution. FML employs the intradermal administration of a fluorescent dye, FITC conjugated to dextran (FITC-dextran), and video fluorescence microscopy techniques to collect high-resolution images. Owing to the limited penetration depth of light at visible wavelengths and tissue scattering, only the initial capillaries within the first 100 to 150 microns of tissue depth can be visualized in humans. In preclinical investigations, the honeycomb-like lymphatic structure in rat and mouse tails can be non-invasively imaged (24, 25). In normal control subjects, FML enables visualization of only a few of the initial lymphatics close to the intradermal depot of FITC dye, while in subjects with lymphedema, the visualized network of initial lymphatics surrounding the injection sites is considerably larger, presumably due to higher pressures in proximal conducting lymphatic vessels that prevent efflux of dye from the initial capillaries into conducting and collecting lymphatic vessels (Figure 2C). The administered fluorescent dye can also penetrate deeper into collecting and conducting lymphatic vessels, where it escapes optical interrogation by microscopy techniques and, in subjects with congenital and acquired lymphedema, can be seen to reappear at tissue surfaces distant to the injection site, due again to higher pressures or blockage in proximal conducting vessels that redirect lymph flow distally as well as into the initial capillary vessels (26–29). Tissue penetration of FML techniques can be enhanced using indocyanine green (ICG), a dye that is approved in humans for intravenous administration, has been used in hepatic

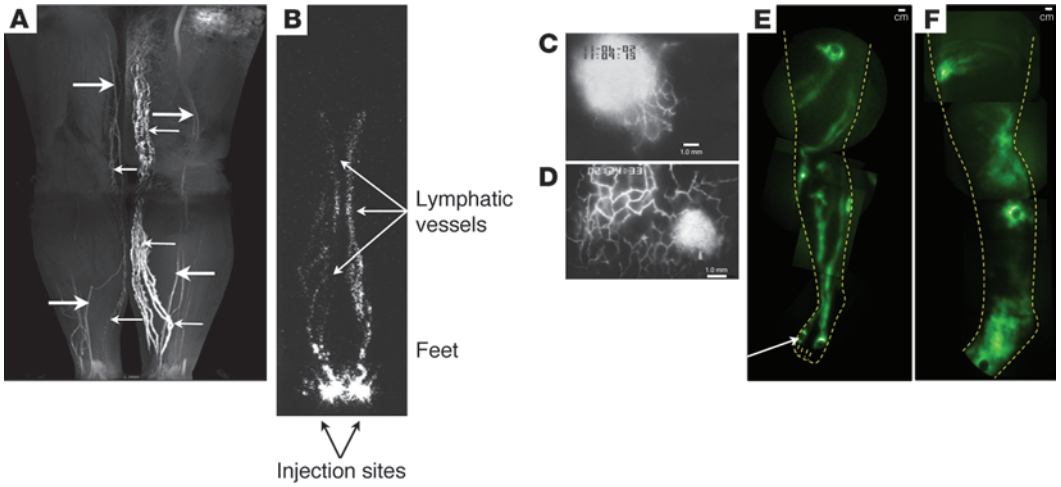

Figure 2
Examples of lymphatic imaging. (**A**) MR lymphography (indirect) of normal (left) and diseased (right) lymphatic structure (thin arrows) following administration of gadopentate dimeglumine. Some enhanced veins are also shown (thick arrows). Reproduced with permission from *PLoS One* (13). (**B**) Lymphoscintigram of lymphatic drainage in the lower extremities (anterior view) following bipedal administration of 99mTc antimony sulfur colloid. Reproduced with permission from *Journal of Nuclear Medicine* (19). (**C** and **D**) FML of FITC-dextran in initial lymphatic capillaries of medial ankle of human normal control subject (**C**) and subject with primary lymphedema (**D**). Reproduced with permission from *Lymphology* (29). (**E** and **F**) NIRF imaging of the lymphatic drainage of an asymptomatic leg (**E**) and a symptomatic leg (**F**) following administration of ICG. Reproduced with permission from *Proceedings of the National Academy of Sciences of the United States of America* (89). Scale bars: 1 mm (**C** and **D**); 1 cm (**E** and **F**).

and cardiovascular testing and retinal angiography, and can be excited by tissue-penetrating near-infrared (NIR) light (>780 nm). While poorly fluorescent, the dye may be used in humans in an off-label, intradermal route of administration for interrogation of the lymphatics. Confocal fluorescence microscopy techniques employing ICG have recently been demonstrated to afford greater resolution to probe the initial lymphatics at tissue depths of up to 200 microns (30).

NIR fluorescence (NIRF) lymphatic imaging, also termed ICG lymphography, is an emerging non-microscopic imaging technology that collects tissue-scattered light to assess conducting and collecting lymphatic vessels at greater penetration depths, but with lower resolution than the initial lymphatics imaged with FML. Upon illumination of tissue surfaces with NIR excitation light, ICG fluorescence is collected using charge-coupled device (CCD) cameras and can be used to visualize the initial lymphatics, collecting and conducting lymphatics, and draining LNs across wide fields of view that can encompass entire limbs (Figure 2, E and F). The majority of studies that employ NIRF imaging with ICG focus on pre-surgical and intraoperative sentinel LNM (SLNM) and dissection (31–33). While investigational camera designs have widely varying sensitivity (34, 35), non-invasive NIRF imaging can detect the lymphatic vasculature located as deep as 3–4 cm beneath the tissue surface with as little as 10 μg of ICG in 0.1 ml in humans (36) using intensified camera technologies, and up to 5 μg of ICG in 10 μl in mice using electron multiplier CCD technology (37–39). In clinical studies, NIRF imaging using ICG has been demonstrated to detect subclinical lymphedema (40, 41) to guide and assess lymphatico-venous anastomosis microsurgery in a case of lower extremity lymphedema (42), and has been found to be superior to lymphoscintigraphy in the diagnosis of lymphedema (43). Because lymphatic vessel reconstitution plays an important role in transplantation, NIRF imaging of the lymphatics with ICG has also been used to assess tissue rejection in an animal model of hind limb transplantation (44), suggesting potential uses in clinical regenerative medicine. Nonetheless, tissue penetration that depends upon the imaging performance of individual camera systems is a limitation, and NIRF imaging cannot be used to visualize the truncal lymphatics in adults and children as can x-ray lymphangiography employing intra-lymphatic contrast agents. Thus, non-invasive NIRF imaging of ICG has been confined to imaging the peripheral lymphatics (including initial, collecting, and conducting) in both humans and animals.

Imaging techniques to assess lymphatic function

Unlike other lymphatic imaging approaches described in Table 1, NIRF lymphatic images can be collected rapidly with millisecond acquisitions (33), allowing for the non-invasive interrogation of function in collecting and conducting lymphatic vessels (40, 45, 46) and the quantitative assessment of the lymph pump frequency and apparent velocity in the collecting and conducting lymphatics of both mice and humans (Supplemental Videos 1 and 2; supplemental material available online with this article; doi:10.1172/JCI71612DS1). The mechanism for lymph pumping, an intrinsic property of the lymphatic muscle, is due in part to the rhythmic constriction/relaxation cycle of vascular smooth muscle cells, called lymphangions, that are bounded by valve leaflets that open and close in an orchestrated manner to mediate unidirectional, efficient lymph flow (reviewed in ref. 47). The lymph pump is thought be controlled by the autonomic nervous system and is critical to tissue fluid homeostasis and immune cell transport. The identification of factors that affect lymphatic pumping is an active area of research that will contribute to the development of

Table 1
Summary of imaging modalities for visualizing the lymphatic vasculature in vivo within small and large animals and humans

Modality	Temporal resolution (acquisition times)	Spatial resolution	Depth resolution	Small animals	Large animals	Humans	Contrast agents	Comments and selected references
X-ray lymphangiography, direct	ms/exposure; requires surgical intervention to cannulate lymphatic vessel	<1 mm	Whole body	No	Yes	Yes	Oily, iodinated agents such as Ethiodol/Lipiodol	Used on a limited basis due to incidence of clinical complications and technical skill required to locate and cannulate lymphatic vessel (9, 112, 113)
X-ray lymphangiography, indirect	ms/exposure	<1 mm	Whole body	No	Yes	Yes	Water-soluble iodinated agents such as Iotasul	(114)
X-ray computed tomography	>20 s/exposure, dependent on region of interest and desired resolution	1–3 mm	Whole body	Limited	Yes	Yes	Water-soluble iodinated agents such as Iopamidal	Visualizes LNs and some larger lymphatic vessels (115, 116)
MRI lymphangiography	>2 min/exposure, dependent on region of interest and desired resolution	0.1–0.3 mm in mice, 1 mm in human	Whole body	Yes	Yes	Yes	Gadolinium or iron oxide–based agents; dendrimer-based macromolecules	Difficult to resolve healthy, intact lymphatic vessels (16, 117–119)
MRI (non-contrast)	Minutes/exposure	1 mm	Whole body	No	Yes	Yes	Unknown	Can only resolve dilated lymphatics filled with stagnant lymph (8)
Lymphoscintigraphy	20–60 min/exposure	~1 cm	Whole body	No	Yes	Yes	Radiolabeled sulfur colloid, radiolabeled dextran; technitium most commonly used isotope	Visualizes large lymphatic vessels and nodes only (20, 23)
FML	Video rates	50 μm	200 μm	Yes	Yes	Yes	FITC-dextran	Visualizes the initial lymphatics near the injection site (25–29)
NIRF	Typically 50–800 ms/image	~200 μm at tissue surface; due to photon scatter, resolution decreases as depth increases, but larger, deeper vessels are visualized	Varies with vessel diameter; larger nodes can be visualized up to 3–4 cm deep	Yes	Yes	Yes	NIRF dyes, Qdots, gene reporters	Initial lymphatics as well as collecting and conducting vessels observed; active lymphatic propulsion observed in small and large animals as well as in humans; photon scattering limits spatial resolution; only off-label use of ICG is currently allowed in humans (31, 35, 37)

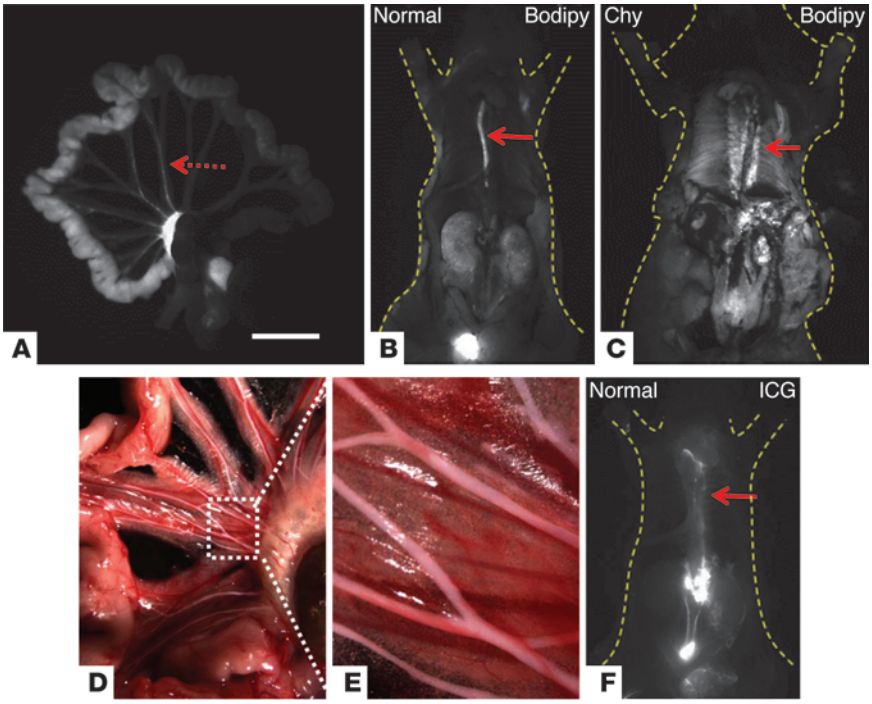

Figure 3
Images of the mesenteric lymphatics, truncal lymphatics, and thoracic duct. (**A**–**C**) In situ imaging of mesenteric lymphatics (dashed arrow) in exteriorized mesentery (**A**) and exposed thoracic duct of mouse following oral gavage of BODIPY FL C_{16} in normal (**B**) and Chy (**C**) mice. Note the leaky thoracic duct in the Chy mouse. (**D**) Mesenteric mouse lymphatics visualized following oral gavage of heavy cream. (**E**) Expanded view of the area within the dashed box in **D**. (**F**) The exposed thoracic duct can also be imaged, although not as clearly, following intradermal administration of ICG in the hind limb. Scale bar: 1 cm.

new pharmacologic strategies to correct lymphatic insufficiency. Lymphatic dysfunction is generally diagnosed based upon onset of late-stage, irresolvable symptoms of edema, chylous ascites, and chylothorax. Early detection of dysfunctional lymphatic transport in asymptomatic patients before onset of symptoms could enable earlier diagnoses and more effective treatments. Indeed, in the specific case of breast cancer–related lymphedema, Gergich and coworkers (48) found that early intervention could improve the outcome of upper extremity lymphedema. Clinical decisions in other conditions/diseases in the areas of wound care, diabetes, cancer care, and peripheral vascular disease might also be improved if the contributory role of the lymphatic function were evaluated through non-invasive imaging techniques.

Because of its high temporal resolution, NIRF imaging has been used to image the lymphatic function and architecture in patients with metastatic cancer (49) and in mouse models of metastasis (39, 50–52). In humans, NIRF lymphatic imaging has been used to show that manual lymphatic drainage therapy directly affects lymphatic pumping in normal healthy adults and in some subjects with early lymphedema (53), thus providing direct evidence of benefit needed by the U.S. Centers for Medicare and Medicaid for continuing coverage of lymphedema treatments (54). The changes in lymph pumping have been non-invasively imaged in preclinical animal models (55) of salt-induced hypertension (56), rheumatoid arthritis (57, 58), acute inflammation (59), and wound healing (60). Furthermore, cytokine-induced changes in lymph pumping, including retrograde lymph flow, have been non-invasively visualized and quantified (59) with results that are consistent with invasive, intravital fluorescence measurements using FITC-dextran (61). Because tissue optical properties limit the utility of visibly excited fluorescent dyes in non-invasive imaging, dyes that can be excited by NIR light offer the most straightforward means to understand which factors affect lymphatic pumping in non-invasive mouse and in human investigations.

Imaging mesenteric and truncal lymphatics

In contrast to the peripheral lymphatics, the mesenteric lymphatics are a major route for dietary lipid uptake and transport, but little is known about the precise mechanisms mediating lipid transport and metabolism. Lipids are absorbed as monoglycerides and fatty acids from the intestinal lumen into the enterocytes, where they are esterified into triglycerides and packaged to form chylomicrons (62, 63). The chylomicrons are too large to enter the blood capillaries and must be taken up by the lacteal lymphatics (Figure 1, route iii), then transported through the lymphatic system to the thoracic duct, where they enter the bloodstream via the subclavian vein. Non-invasive, direct imaging of the mesenteric lymphatic system is not currently possible in animals or humans due to its inaccessible, anatomic location and lack of an imaging agent that is readily taken up by the lacteals. Mesenteric lymphatic vessels in mice and rats have been imaged in situ using intravital optical microscopy after mesenteric loops were exteriorized (47).

Fluorescent lipid analogs provide a way to invasively image mesenteric lymphatics and lipid metabolism. A fluorescently labeled 16-carbon-chain fatty acid, 4,4-difluoro-5,7-dimethyl-4-bora-3a,4a-diaza-s-indacene-3-hexadecanoic acid (BODIPY FL C_{16}), has been used as a lipid tracer to invasively study lymphatic architecture and function in the mesentery lymphatics (Figure 3, A–C, and ref. 64). After oral gavage, BODIPY FL C_{16} is taken up by lymphatic lacteals in the villi of the small intestine and packaged along with triglycerides to form fluorescent chylomicrons. Thus, architectural and functional changes of mesenteric lymphatics and the thoracic duct can be invasively imaged in animal models of diseases, including *Prox1*-associated obesity (65), ovarian cancer (66), liver cirrhosis (67), and lymphedema (Figure 3C). In humans, the thoracic duct can be visualized intraoperatively following oral ingestion of heavy cream (Figure 3, D and E, and ref. 68) or through opacification of the thoracic duct following pedal (69) or intranodal (70, 71) lymphangiography. In swine and

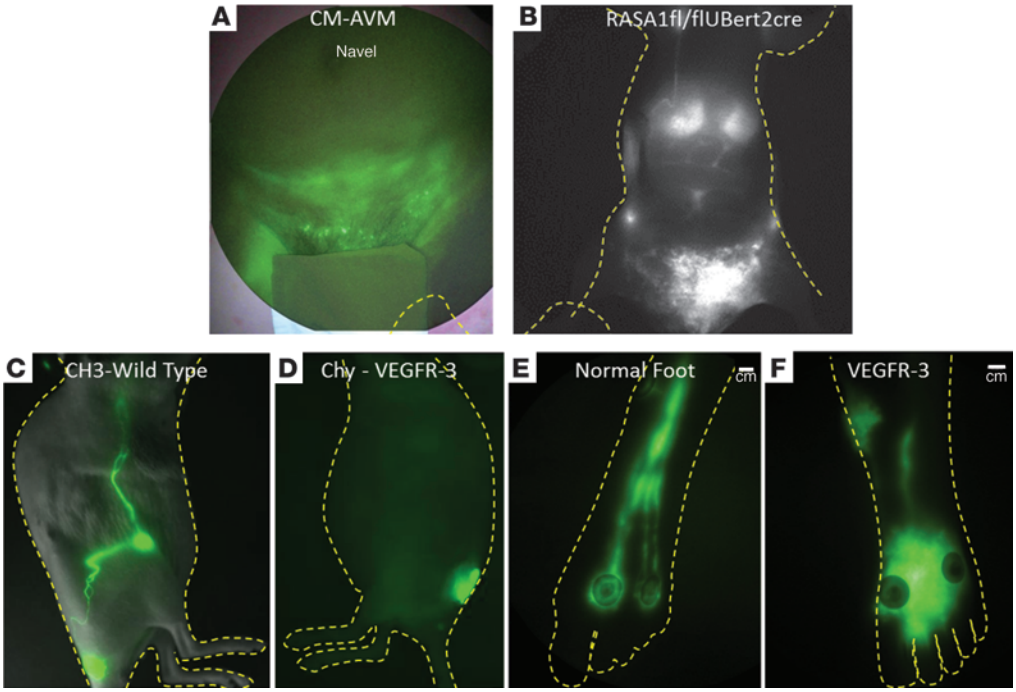

Figure 4
Comparison of lymphatic phenotypes in humans and animal models of disease. (**A**) The drainage of ICG from the lower extremity lymphatics into the abdomen in a subject diagnosed with Parkes Weber syndrome, associated with an inactivating mutation in *RASA1*. (**B**) The drainage of ICG into the abdominal cavity of a *Rasa1* knockout mouse (*Rasa1*$^{fl/fl}$*/ubErt2-cre*) exhibiting lymphatic hyperplasia. Reproduced with permission from *Proceedings of the National Academy of Sciences of the United States of America* (89). (**C** and **D**) Lymphatic drainage in a WT mouse (**C**) and a Chy mouse (**D**) with a *Vegfr3* loss-of-function mutation. (**E** and **F**) Similar phenotypes are observed in a normal human foot (**E**) and the foot of a human subject with a *VEGFR3* mutation (**F**).

mice, the thoracic duct has been visualized intraoperatively using fluorescence imaging following administration of ICG in the hind limbs (Figure 3F and ref. 72), but tissue penetration issues prevent the non-invasive visualization of the thoracic duct in adult human subjects and currently limit non-invasive visualization in infants and animal models.

Emerging imaging agents for the lymphatics

FITC and ICG are the only visible and NIR excited fluorescent lymphatic agents used in human studies, but new fluorescent imaging agents have emerged for preclinical investigations and may be translatable to humans in the future. Fluorescent contrast agents that are brighter and may be more suitable for non-invasive imaging include quantum dots (Qdots) (73) and a NIRF-labeled, albumin-binding domain peptide that measures protein uptake and lymphatic transport (74). Molecular imaging agents that target the lymphatic vasculature are also in development. Using phage screening, Laakkonen et al. identified and fluorescently labeled a cyclic 9-amino-acid peptide, LyP1, which homes to lymphatic endothelial cells (LECs) and tumor cells (75). LYVE1 is a major receptor for ECM glycosaminoglycan hyaluronan on LECs (76) and has been fluorescently labeled with NIRF dye to show staining of lymphatic vessels in swine (45). Fluorescently labeling (77), radiolabeling (78), or conjugating magnetic nanoparticles (79) to a LYVE1 antibody has allowed investigators to visualize lymphatics through fluorescence, PET, and molecular MRI. Fluorescently labeled antibodies targeting CD11b and GR1 have allowed for imaging of immune cell migration within lymphatic vessels using intravital fluorescence imaging (58). Dendritic cell trafficking to LNs has been performed using non-invasive MRI techniques with ultra-small iron oxide particles (USPIOs) that are administered intradermally (80).

Gene reporters for lymphatic imaging in transgenic mouse models of human disease

Gene reporter imaging used in transgenic mouse models of human disease involves the use of fluorescent or bioluminescent reporters for visualizing lymphatic vessels, usually with intravital imaging techniques. Expressed under the control of the LEC gene marker *Prox1*, the fluorescent proteins GFP (81), mOrange (82), and mTomato (83) have been used in transgenic animals to visualize lymphatic vessels with intravital microscopy. The role of NO in lymphatic contractile activity and immune responses was probed using mice that express the fluorescent protein DsRed under the control of a smooth muscle cell promoter (*Acta2*) (61). More recently, animals have been developed to express the dual reporter, EGFP-LUC, consisting of EGFP and luminescent LUC reporters under the control of *Vegfr3*. In this model, high-resolution intravital fluorescence imaging is used to collect fluorescence from EGFP at the study endpoint, while lower-resolution, non-invasive bioluminescence imaging is used to longitudinally assess lymphatic vessels in vivo during development, wound healing, inflammation, and tumor metastasis (84). The dual reporter approach marries imaging information from high-resolution intravital microscopy at the endpoint of the animal study, with low-resolution, non-invasive

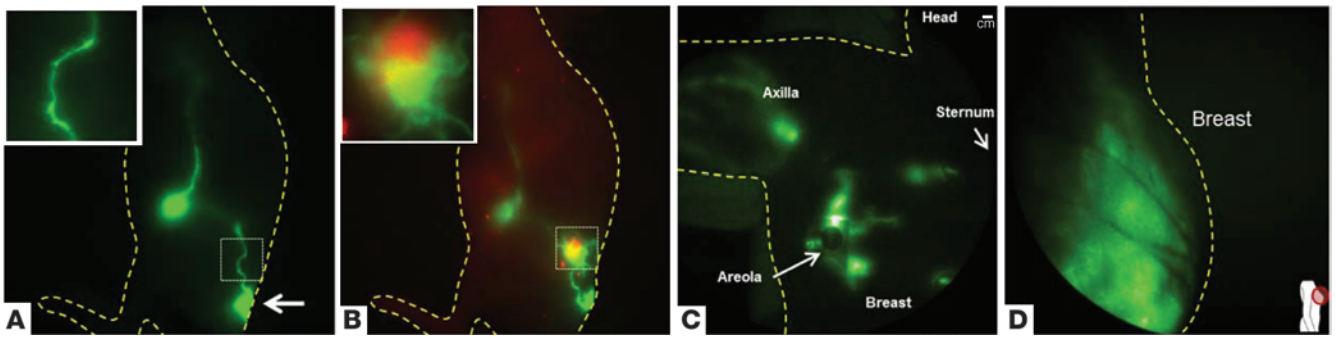

Figure 5
Images of the effect of breast carcinoma on lymphatic structure. (**A**) A baseline NIRF image of murine lymphatics prior to inoculation of IBC cells (SUM149) transfected with the iRFP gene reporter. The inset figure is a magnification of the lymphatic structure proximal the site of ICG administration (arrow). (**B**) An overlay of a NIRF image (green) of the lymphatics over a non-invasive iRFP image of the gene reporters in the primary tumor 21 days post-inoculation (p.i.) of the SUM149 cells. Note the reorganization of the lymphatics surrounding the tumor (inset). (**C** and **D**) Abnormal lymphatic phenotype in a subject with IBC (**C**) and invasive ductal carcinoma (**D**) following administration of ICG in the arm, the areola, and the quadrants of the breast. Reproduced with permission from *Biomedical Optics Express* (111).

bioluminescence to longitudinally assess lymphatic remodeling responses. In contrast to the visibly excited fluorescent gene reporters, newer, far-red–shifted fluorescent gene reporters (85, 86) can be imaged non-invasively and longitudinally in whole animals (our unpublished observations and ref. 87), suggesting they may extend fluorescent gene reporter imaging beyond intravital imaging and facilitate non-invasive, longitudinal imaging of lymphatic remodeling. To date, these far-red fluorescent gene reporters have not been employed in any transgenic animal models, but could dramatically affect future preclinical study of the lymphatics.

Phenotyping human lymphatic disorders in mice and man

Table 1 is a summary of the non-invasive imaging techniques used both in mice and humans. The ability to directly relate lymphatic phenotypes between human subjects and transgenic animal models of lymphatic disorders is an important advantage unique to fluorescence imaging, particularly NIRF and FML. For example, using NIRF imaging, the abnormal, hyperplastic lymphatic phenotype associated with an inducible knockout of *Rasa1* in a transgenic mouse model (88) was recently associated with that of a human subject with the rare syndromic disorder of capillary malformation–arteriovenous malformation, which is caused by an inactivating mutation in *RASA1* (Figure 4, A and B). The patient exhibited unusually dilated lymphatics in the unaffected lower extremity compared with normal subjects (Supplemental Videos 2 and 3) (89). Abnormal phenotypes of defective drainage patterns, hypoplasia, and retrograde lymph flow have also been imaged in *Prox1* heterozygous mice (38) and in Chy mice with a loss-of-function *Vegfr3* mutation (90) using NIRF lymphatic imaging. In the latter, NIRF imaging of the hypoplastic lymphatic phenotype in the Chy mouse and a subject with a *VEGFR3* mutation are strikingly similar (Figure 4, C–F). FML also confirms the lack of initial lymphatics in Milroy's disease, which is associated with *VEGFR3* mutations (91). The Chy model also provides an animal model for developing new pharmacologic strategies to stimulate lymphatic vessel development in human lymphedema (92). In a preclinical study, Tammela and coworkers (93) used FITC-dextran imaging to demonstrate enhanced regrowth of lymphatic vessels and improved lymphatic function across sites of LN dissection following *VEGFC/D* gene therapy. Thus, fluorescence lymphatic imaging can provide a preclinical method for directly assessing emerging molecular therapeutics on the initial, conducting, and collecting peripheral lymphatics (51).

Lymphatic imaging for cancer diagnostics and therapeutic development

Recent research has focused on the development of new imaging methods for SLNM in cancer patients to augment lymphoscintigraphy, thereby improving staging by imaging only cancer-positive LNs, and to assess tumor-associated lymphangiogenesis.

SLNM is currently conducted clinically with lymphoscintigraphy and blue dye, the latter of which is visually apparent intraoperatively, to identify tumor-draining LNs for subsequent biopsy. Clinical approaches proposed for improved SLNM include intraoperative use of ICG (94) and a recently approved, macrophage-targeted, radiolabeled sugar (tilmanocept) (95, 96) that has also been labeled with a NIRF dye (97) or a radionuclide/NIRF conjugate (98). Other investigational approaches for SLNM conducted in preclinical studies have employed QDots (99), MR lymphangiography with Gadolinium-based contrast agents (100), and gold nanorods that were tracked using photoacoustic imaging (101).

While the lacteals of the mesenteric lymphatics and the initial lymphatics of the peripheral circulation provide the physiologic points of entry into the lymphatic vasculature, intravenously administered contrast agents can enter into the lymphatics via the high-endothelial venules of LNs (Figure 1, route iv), as well as through the reticuloendothelial system. For example, when USPIOs, used as contrast agents in MRI, are administered intravenously, either they gain access to the interstitium, are taken up by the lymphatics and transit to LNs or are captured by mononuclear phagocytic cells that then hone to LNs (reviewed in ref. 102). Upon accumulation of the USPIOs in draining LNs, a reduced signal intensity on T2/T2* weighted images creates negative contrast of draining LNs, allowing non-invasive detection. However, when metastases block drainage, the LN appears bright on the T2/T2* MRI, enabling potential differential identification of cancer-positive over cancer-negative LNs (103). Gadofosvet trisodium (reviewed in ref. 104) has also recently been employed as a MR-positive T1 contrast agent for axillary LNs after intravenous administration (105).

The ability to non-invasively image cancer-positive LNs could obviate the need for LN dissection for the purposes of cancer staging. Molecularly specific imaging for detection of cancer-positive LNs has been proposed, employing intravenous administration of radiolabeled and fluorescently labeled antibodies for targeting cancer cells (106, 107). These antibody-based approaches possess high specificity to the cancer-specific antigen, but also typically contain the Fc domain to which immune cells resident within LNs can bind (108). As a result, molecular imaging approaches that employ a full antibody as opposed to antibody fragments or Fc-silenced antibodies are likely to suffer from false positives and reduced specificity. To date, there remains no viable means to accurately detect cancer-positive LNs with a targeted molecular imaging agent.

The use of imaging to assess the interaction between metastasizing cancer cells and the host lymphatic vasculature represents a critical cancer research tool. Longitudinal imaging of functional and architectural lymphatic changes in patients (49) and in animal models of cancer provides a window for assessing the role of the lymphatics in cancer progression and metastasis (39, 51, 52). Preclinical imaging studies to track the migration of cancer cells marked with a fluorescent gene reporter have been pioneered by a number of investigators (77, 109). For example, the leaky and tortuous tumor lymphatic vessel phenotype around a tumor less than 2 mm in diameter can be readily imaged (Figure 5, A and B) using the far red fluorescent protein, iRFP, which is stably expressed by a human inflammatory breast cancer (IBC) cell line and ICG lymphatic imaging (110). IBC is rare in humans but is known to infiltrate the skin and lymphatic vessels of the breast, thus partially obstructing subdermal lymphatics and causing breast lymphedema. Figure 5, C and D, provides an example of NIRF lymphatic imaging of women diagnosed with IBC and invasive ductal carcinoma with observed abnormal lymphatic drainage suggesting lymphatic reorganization of the dermal lymphatics (111).

Conclusions

The armamentarium of lymphatic imaging techniques for clinical research investigations and longitudinal imaging in animal models of human disease has accelerated biological discoveries and may hasten their clinical translation. In less than a decade, significant advances in NIRF lymphatic imaging, nanotechnology-based MRI agents, and gene reporter technologies have provided new tools for interrogating the diverse functions of the lymphatic vasculature. For example, lymphatic imaging may be useful in determining the impact of specific signaling pathways when used in conjunction with transgenic animal models of human disease and enable visualization of the effects of therapeutic interventions. The development of transgenic models using far-red fluorescent gene reporters could contribute to lymphatic research by enabling non-invasive imaging of dynamic lymphatic processes and pathologies. Because of the inherent plasticity of the lymphatic system, longitudinal imaging techniques both for preclinical and clinical investigations need to be further developed, particularly for mesenteric and truncal lymphatics. While not all lymphatic imaging modalities are amenable to both clinical and preclinical investigation, their strategic combination provides opportunities for biological discovery and clinical translation in lymphatic research. The clinical application of lymphatic imaging techniques in cancer care, cancer survivorship, chronic wounds, peripheral vascular disease, and other conditions in which the lymphatics potentially mediate clinical outcomes may enable more efficient diagnoses and better treatments.

Acknowledgments

This work was supported in parts by NIH grants R01 HL092923 (to E.M. Sevick-Muraca), R01 CA128919 (to E.M. Sevick-Muraca), and R21 CA159293 (to S. Kwon). The authors acknowledge the assistance of Jessica Nollkamper in the preparation of the manuscript.

Address correspondence to: Eva M. Sevick-Muraca, Center for Molecular Imaging, The Brown Foundation Institute of Molecular Medicine, University of Texas Health Science Center, 1825 Pressler Street, SRB 330A, Houston, Texas 77030, USA. Phone: 713.500.3560; Fax: 713.500.3561; E-mail: eva.sevick@uth.tmc.edu.

1. Jaffer FA, Libby P, Weissleder R. Molecular imaging of cardiovascular disease. *Circulation*. 2007;116(9):1052–1061.
2. Clement O, Luciani A. Imaging the lymphatic system: possibilities and clinical applications. *Eur Radiol*. 2004;14(8):1498–1507.
3. Sharma R, Wendt JA, Rasmussen JC, Adams KE, Marshall MV, Sevick-Muraca EM. New horizons for imaging lymphatic function. *Ann N Y Acad Sci*. 2008;1131:13–36.
4. Lucarelli RT, Ogawa M, Kosaka N, Turkbey B, Kobayashi H, Choyke PL. New approaches to lymphatic imaging. *Lymphat Res Biol*. 2009;7(4):205–214.
5. Zhang F, Niu G, Lu G, Chen X. Preclinical lymphatic imaging. *Mol Imaging Biol*. 2011;13(4):599–612.
6. Proulx ST, Detmar M. Molecular mechanisms imaging of lymphatic metastasis. *Exp Cell Res*. 2013;S0014-4827
7. Chen SL, Iddings DM, Scheri RP, Bilchik AJ. Lymphatic mapping and sentinel node analysis: current concepts and applications. *CA Cancer J Clin*. 2006;56(5):292–309.
8. Liu N, Wang C, Sun M. Noncontrast three-dimensional magnetic resonance imaging vs lymphoscintigraphy in the evaluation of lymph circulation disorders: A comparative study. *J Vasc Surg*. 2005;41(1):69–75.
9. Kinmonth JB. Lymphangiography in man; a method of outlining lymphatic trunks at operation. *Clin Sci (Lond)*. 1952;11(1):13–20.
10. Mennini ML, Catalano C, Del Monte M, Fraioli F. Computed tomography and magnetic resonance imaging of the thoracic lymphatic system. *Thorac Surg Clin*. 2012;22(2):155–160.
11. Lohrmann C, Foeldi E, Langer M. Indirect magnetic resonance lymphangiography in patients with lymphedema preliminary results in humans. *Eur J Radiol*. 2006;59(3):401–406.
12. Lohrmann C, Foeldi E, Langer M. Diffuse lymphangiomatosis with genital involvement — evaluation with magnetic resonance lymphangiography. *Urol Oncol*. 2011;29(5):515–522.
13. Lu Q, et al. MR lymphography of lymphatic vessels in lower extremity with gynecologic oncology-related lymphedema. *PLoS One*. 2012;7(11):e50319.
14. Notohamiprodjo M, et al. MR lymphangiography at 3.0 T: correlation with lymphoscintigraphy. *Radiology*. 2012;264(1):78–87.
15. Kobayashi H, et al. Comparison of dendrimer-based macromolecular contrast agents for dynamic micro-magnetic resonance lymphangiography. *Magn Reson Med*. 2003;50(4):758–766.
16. Kobayashi H, et al. Lymphatic drainage imaging of breast cancer in mice by micro-magnetic resonance lymphangiography using a nano-size paramagnetic contrast agent. *J Natl Cancer Inst*. 2004;96(9):703–708.
17. Sena LM, et al. Magnetic resonance lymphangiography with a nano-sized gadolinium-labeled dendrimer in small and large animal models. *Nanomedicine (Lond)*. 2010;5(8):1183–1191.
18. Kiryu S, et al. Interstitial MR lymphography in mice: comparative study with gadofluorine 8, gadofluorine M, and gadofluorine P. *Magn Reson Med Sci*. 2012;11(2):99–107.
19. Szuba A, Shin WS, Strauss HW, Rockson S. The third circulation: radionuclide lymphoscintigraphy in the evaluation of lymphedema. *J Nucl Med*. 2003;44(1):43–57.
20. Scarsbrook AF, Ganeshan A, Bradley KM. Pearls and pitfalls of radionuclide imaging of the lymphatic system. Part 2: evaluation of extremity lymphoedema. *Br J Radiol*. 2007;80(951):219–226.
21. Zimmerman H, Fessa CK, Rossleigh MA, Wegner EA. Lymphoscintigraphy of lower limb edema. *Clin Nucl Med*. 2012;37(4):411–415.
22. Tartaglione G, et al. Intradermal lymphoscintigraphy at rest and after exercise: a new technique for the functional assessment of the lymphatic system in patients with lymphoedema. *Nucl Med Commun*. 2010;31(6):547–551.
23. Modi S, Stanton AW, Mortimer PS, Levick JR. Clinical assessment of human lymph flow using removal rate constants of interstitial macromolecules: a critical review of lymphoscintigraphy. *Lymphat Res Biol*. 2007;5(3):183–202.
24. Leu AJ, Berk DA, Yuan F, Jain RK. Flow velocity in the superficial lymphatic network of the mouse

tail. *Am J Physiol*. 1994;267(4 pt 2):H1507–H1513.
25. Leu AJ, et al. Absence of functional lymphatics within a murine sarcoma: a molecular and functional evaluation. *Cancer Res*. 2000;60(16):4324–4327.
26. Bollinger A, Jäger K, Sgier F, Seglias J. Fluorescence microlymphography. *Circulation*. 1981; 64(6):1195–1200.
27. Stanton AW, Kadoo P, Mortimer PS, Levick JR. Quantification of the initial lymphatic network in normal human forearm skin using fluorescence microlymphography and stereological methods. *Microvasc Res*. 1997;54(2):156–163.
28. Mellor RH, et al. Enhanced cutaneous lymphatic network in the forearms of women with postmastectomy oedema. *J Vasc Res*. 2000;37(6):501–512.
29. Bollinger A, Amann-Vesti BR. Fluorescence microlymphography: diagnostic potential in lymphedema and basis for the measurement of lymphatic pressure and flow velocity. *Lymphology*. 2007;40(2):52–62.
30. Jonak C, et al. Intradermal indocyanine green for in vivo fluorescence laser scanning microscopy of human skin: a pilot study. *PLoS One*. 2011;6(8):e23972.
31. Polom K, et al. Current trends and emerging future of indocyanine green usage in surgery and oncology: a literature review. *Cancer*. 2011;117(21):4812–4822.
32. Schaafsma BE, et al. The clinical use of indocyanine green as a near-infrared fluorescent contrast agent for image-guided oncologic surgery. *J Surg Oncol*. 2011;104(3):323–332.
33. Sevick-Muraca EM. Translation of near-infrared fluorescence imaging technologies: emerging clinical applications. *Annu Rev Med*. 2012;63:217–231.
34. Zhu B, Rasmussen JC, Sevick-Muraca EM. A matter of collection and detection for intraoperative and noninvasive near-infrared fluorescence molecular imaging: To see or not to see? *Med Physic*. 2014;41:022105. doi:10.1118/1.4862514.
35. Marshall MV, et al. Near-Infrared Fluorescence Imaging in Humans with Indocyanine Green: A Review and Update. *Open Surg Oncol J*. 2010;2(2):12–25.
36. Sevick-Muraca EM, et al. Imaging of lymph flow in breast cancer patients after microdose administration of a near-infrared fluorophore: feasibility study. *Radiology*. 2008;246(3):734–741.
37. Kwon S, Sevick-Muraca EM. Noninvasive quantitative imaging of lymph function in mice. *Lymphat Res Biol*. 2007;5(4):219–231.
38. Kwon S, Sevick-Muraca EM. Mouse phenotyping with near-infrared fluorescence lymphatic imaging. *Biomed Opt Express*. 2011;2(6):1403–1411.
39. Kwon S, et al. Direct visualization of changes of lymphatic function and drainage pathways in lymph node metastasis of B16F10 melanoma using near-infrared fluorescence imaging. *Biomed Opt Express*. 2013;4(6):967–977.
40. Rasmussen JC, et al. Lymphatic imaging in humans with near-infrared fluorescence. *Curr Opin Biotechnol*. 2009;20(1):74–82.
41. Mihara M, et al. Predictive lymphatic mapping: a method for mapping lymphatic channels in patients with advanced unilateral lymphedema using indocyanine green lymphography [published online ahead of print March 12, 2013]. *Ann Plast Surg*. doi:10.1097/SAP.0b013e31826a18b1.
42. Mihara M, et al. Lower limb lymphedema treated with lymphatico-venous anastomosis based on pre-and intraoperative icg lymphography and non-contact vein visualization: a case report. *Microsurgery*. 2012;32(3):227–230.
43. Mihara M, et al. Indocyanine green (ICG) lymphography is superior to lymphoscintigraphy for diagnostic imaging of early lymphedema of the upper limbs. *PLoS One*. 2012;7(6):e38182.
44. Buretta KJ, et al. Near-infrared lymphography as a minimally invasive modality for imaging lymphatic reconstitution in a rat orthotopic hind limb transplantation model. *Transpl Int*. 2013;26(9):928–937.
45. Sharma R, et al. Quantitative imaging of lymph function. *Am J Physiol Heart Circ Physiol*. 2007; 292(6):H3109–H3118.
46. Unno N, et al. A novel method of measuring human lymphatic pumping using indocyanine green fluorescence lymphography. *J Vasc Surg*. 2010; 52(4):946–952.
47. Muthuchamy M, Zawieja D. Molecular regulation of lymphatic contractility. *Ann N Y Acad Sci*. 2008;1131:89–99.
48. Stout Gergich NL, et al. Preoperative assessment enables the early diagnosis and successful treatment of lymphedema. *Cancer*. 2008;112(12):2809–2819.
49. Rasmussen JC, Kwon S, Sevick-Muraca EM, Cormier JN. The role of lymphatics in cancer as assessed by near-infrared fluorescence imaging. *Ann Biomed Eng*. 2012;40(2):408–421.
50. Kwon S, Sevick-Muraca EM. Functional lymphatic imaging in tumor-bearing mice. *J Immunol Methods*. 2010;360(1–2):167–172.
51. Gogineni A, et al. Inhibition of VEGF-C modulates distal lymphatic remodeling and secondary metastasis. *PLoS One*. 2013;8(7):e68755.
52. Proulx ST, et al. Use of a PEG-conjugated bright near-infrared dye for functional imaging of rerouting of tumor lymphatic drainage after sentinel lymph node metastasis. *Biomaterials*. 2013;34(21):5128–5137.
53. Tan IC, et al. Assessment of lymphatic contractile function after manual lymphatic drainage using near-infrared fluorescence imaging. *Arch Phys Med Rehabil*. 2011;92(5):756–764 e751.
54. Oremus M, Walker K, Dayes I, Raina P. Diagnosis and treatment of secondary lymphedema. technology assessment report. Baltimore, Maryland, USA: Medicare Evidence Development & Coverage Advisory Committee meeting, Centers for Medicare & Medicaid Services; November 18, 2009. Report No.: Project ID: LYMT0908.
55. Robinson HA, et al. Non-invasive optical imaging of the lymphatic vasculature of a mouse. *J Vis Exp*. 4326;2013(73):e4326.
56. Kwon S, Agollah GD, Chan W, Sevick-Muraca EM. Altered lymphatic function and architecture in salt-induced hypertension assessed by near-infrared fluorescence imaging. *J Biomed Opt*. 2012;17(8):080504–080501.
57. Zhou Q, et al. Near-infrared lymphatic imaging demonstrates the dynamics of lymph flow and lymphangiogenesis during the acute versus chronic phases of arthritis in mice. *Arthritis Rheum*. 2010;62(7):1881–1889.
58. Li J, et al. Efficacy of B cell depletion therapy for murine joint arthritis flare is associated with increased lymphatic flow. *Arthritis Rheum*. 2013;65(1):130–138.
59. Aldrich MB, Sevick-Muraca EM. Cytokines are systemic effectors of lymphatic function in acute inflammation. *Cytokine*. 2013;64(1):362–369.
60. Hall MA, Robinson H, Chan W, Sevick-Muraca EM. Detection of lymphangiogenesis by near-infrared fluorescence imaging and responses to VEGF-C during healing in a mouse full-dermis thickness wound model. *Wound Repair Regen*. 2013; 21(4):604–615.
61. Liao S, et al. Impaired lymphatic contraction associated with immunosuppression. *Proc Natl Acad Sci U S A*. 2011;108(46):18784–18789.
62. Dixon JB. Mechanisms of chylomicron uptake into lacteals. *Ann N Y Acad Sci*. 2010;1:E52–E57.
63. Kindel T, Lee DM, Tso P. The mechanism of the formation and secretion of chylomicrons. *Atheroscler Suppl*. 2010;11(1):11–16.
64. Kassis T, et al. Dual-channel in-situ optical imaging system for quantifying lipid uptake and lymphatic pump function. *J Biomed Opt*. 2012;17(8):086005.
65. Harvey NL, et al. Lymphatic vascular defects promoted by Prox1 haploinsufficiency cause adult-onset obesity. *Nat Genet*. 2005;37(10):1072–1081.
66. Jeon BH, et al. Profound but dysfunctional lymphangiogenesis via vascular endothelial growth factor ligands from CD11b+ macrophages in advanced ovarian cancer. *Cancer Res*. 2008;68(4):1100–1109.
67. Ribera J, et al. Increased nitric oxide production in lymphatic endothelial cells causes impairment of lymphatic drainage in cirrhotic rats. *Gut*. 2013;62(1):138–145.
68. Shackcloth MJ, Poullis M, Lu J, Page RD. Preventing of chylothorax after oesophagectomy by routine pre-operative administration of oral cream. *Eur J Cardiothorac Surg*. 2001;20(5):1035–1036.
69. Cope C, Kaiser LR. Management of unremitting chylothorax by percutaneous embolization and blockage of retroperitoneal lymphatic vessels in 42 patients. *J Vasc Interv Radiol*. 2002;13(11):1139–1148.
70. Nadolski GJ, Itkin M. Thoracic duct embolization for nontraumatic chylous effusion: experience in 34 patients. *Chest*. 2013;143(1):158–163.
71. Parvinian A, et al. Ultrasound-guided intranodal lymphangiography followed by thoracic duct embolization for treatment of post-operative bilateral chylothorax. *Head Neck*. 2014;36(2):E21–E24.
72. Ashitate Y, et al. Near-infrared fluorescence imaging of thoracic duct anatomy and function in open surgery and video-assisted thoracic surgery. *J Thorac Cardiovasc Surg*. 2011;142(1):31–32.
73. Kosaka N, Mitsunaga M, Choyke PL, Kobayashi H. In vivo real-time lymphatic draining using quantum-dot optical imaging in mice. *Contrast Media Mol Imaging*. 2013;8(1):96–100.
74. Davies-Venn CA, et al. Albumin-binding domain conjugate for near-infrared fluorescence lymphatic imaging. *Mol Imaging Biol*. 2012;14(3):301–314.
75. Laakkonen P, Porkka K, Hoffman JA, Ruoslahti E. A tumor-homing peptide with a targeting specificity related to lymphatic vessels. *Nat Med*. 2002;8(7):751–755.
76. Banerji S, et al. LYVE-1, a new homologue of the CD44 glycoprotein, is a lymph-specific receptor for hyaluronan. *J Cell Biol*. 1999;144(4):789–801.
77. McElroy M, et al. Fluorescent LYVE-1 antibody to image dynamically lymphatic trafficking of cancer cells in vivo. *J Surg Res*. 2009;151(1):68–73.
78. Mumprecht V, Detmar M. In vivo imaging of lymph node lymphangiogenesis by immunopositron emission tomography. *Methods Mol Biol*. 2013;961:129–140.
79. Guo Q, et al. Mouse lymphatic endothelial cell targeted probes: anti-LYVE-1 antibody-based magnetic nanoparticles. *Int J Nanomedicine*. 2013;8:2273–2284.
80. Baumjohann D, et al. In vivo magnetic resonance imaging of dendritic cell migration into the draining lymph nodes of mice. *Eur J Immunol*. 2006;36(9):2544–2555.
81. Choi I, et al. Visualization of lymphatic vessels by Prox1-promoter directed GFP reporter in a bacterial artificial chromosome-based transgenic mouse. *Blood*. 2011;117(1):362–365.
82. Hagerling R, et al. Intravital two-photon microscopy of lymphatic vessel development and function using a transgenic Prox1 promoter-directed mOrange2 reporter mouse. *Biochem Soc Trans*. 2011;39(6):1674–1681.
83. Truman LA, et al. ProxTom lymphatic vessel reporter mice reveal Prox1 expression in the adrenal medulla, megakaryocytes, and platelets. *Am J Pathol*. 2012;180(4):1715–1725.
84. Martinez-Corral I, et al. In vivo imaging of lymphatic vessels in development, wound healing, inflammation, and tumor metastasis. *Proc Natl Acad Sci U S A*. 2012;109(16):6223–6228.
85. Shu X, et al. Mammalian expression of infrared fluorescent proteins engineered from a bacterial phytochrome. *Science*. 2009;324(5928):804–807.
86. Shcherbakova DM, Verkhusha VV. Near-infrared fluorescent proteins for multicolor in vivo imag-

ing. *Nat Methods*. 2013;10(8):751–754.
87. Lu Y, et al. In vivo imaging of orthotopic prostate cancer with far-red gene reporter fluorescence tomography and in vivo and ex vivo validation. *J Biomed Opt*. 2013;18(10):101305.
88. Lapinski PE, et al. RASA1 maintains the lymphatic vasculature in a quiescent functional state in mice. *J Clin Invest*. 2012;122(2):733–747.
89. Burrows PE, et al. Lymphatic abnormalities are associated with RASA1 gene mutations in mouse and man. *Proc Natl Acad Sci U S A*. 2013; 110(21):8621–8626.
90. Karlsen TV, et al. Minimally invasive quantification of lymph flow in mice and rats by imaging depot clearance of near-infrared albumin. *Am J Physiol Heart Circ Physiol*. 2012;302(2):H391–H401.
91. Bollinger A, Isenring G, Franzeck UK, Brunner U. Aplasia of superficial lymphatic capillaries in hereditary and connatal lymphedema (Milroy's disease). *Lymphology*. 1983;16(1):27–30.
92. Karkkainen MJ, et al. A model for gene therapy of human hereditary lymphedema. *Proc Natl Acad Sci U S A*. 2001;98(22):12677–12682.
93. Tammela T, et al. Therapeutic differentiation and maturation of lymphatic vessels after lymph node dissection and transplantation. *Nat Med*. 2007;13(12):1458–1466.
94. Vahrmeijer AL, et al. Image-guided cancer surgery using near-infrared fluorescence. *Nat Rev Clin Oncol*. 2013;10(9):507–518.
95. Vera DR, Wallace AM, Hoh CK, Mattrey RF. A synthetic macromolecule for sentinel node detection: (99m)Tc-DTPA-mannosyl-dextran. *J Nucl Med*. 2001;42(6):951–959.
96. Sondak VK, et al. Combined analysis of phase III trials evaluating [(9)(9)mTc]tilmanocept and vital blue dye for identification of sentinel lymph nodes in clinically node-negative cutaneous melanoma. *Ann Surg Oncol*. 2013;20(2):680–688.
97. Emerson DK, et al. A receptor-targeted fluorescent radiopharmaceutical for multireporter sentinel lymph node imaging. *Radiology*. 2012;265(1):186–193.
98. Ting R, et al. Fast 18F labeling of a near-infrared fluorophore enables positron emission tomography and optical imaging of sentinel lymph nodes. *Bioconjug Chem*. 2010;21(10):1811–1819.
99. Kim S, et al. Near-infrared fluorescent type II quantum dots for sentinel lymph node mapping. *Nat Biotechnol*. 2004;22(1):93–97.
100. Kobayashi H, et al. Delivery of gadolinium-labeled nanoparticles to the sentinel lymph node: comparison of the sentinel node visualization and estimations of intra-nodal gadolinium concentration by the magnetic resonance imaging. *J Control Release*. 2006;111(3):343–351.
101. Song KH, Kim C, Maslov K, Wang LV. Noninvasive in vivo spectroscopic nanorod-contrast photoacoustic mapping of sentinel lymph nodes. *Eur J Radiol*. 2009;70(2):227–231.
102. Elias A,Tsourkas A. Imaging circulating cells and lymphoid tissues with iron oxide nanoparticles. *Hematology Am Soc Hematol Educ Program*. 2009;720–726.
103. Harisinghani MG, et al. Noninvasive detection of clinically occult lymph-node metastases in prostate cancer. *N Engl J Med*. 2003;348(25):2491–2499.
104. Sabach AS, et al. Gadofosveset trisodium: abdominal and peripheral vascular applications. *AJR Am J Roentgenol*. 2013;200(6):1378–1386.
105. Schipper RJ, et al. Noninvasive nodal staging in patients with breast cancer using gadofosveset-enhanced magnetic resonance imaging: a feasibility study. *Invest Radiol*. 2013;48(3):134–139.
106. Hall MA, et al. Comparison of mAbs targeting epithelial cell adhesion molecule for the detection of prostate cancer lymph node metastases with multimodal contrast agents: quantitative small-animal PET/CT and NIRF. *J Nucl Med*. 2012;53(9):1427–1437.
107. Heath CH, et al. Use of panitumumab-IRDye800 to image cutaneous head and neck cancer in mice. *Otolaryngol Head Neck Surg*. 2013;148(6):982–990.
108. Fischman AJ, et al. Localization of Fc and Fab fragments of nonspecific polyclonal IgG at focal sites of inflammation. *J Nucl Med*. 1990;31(7):1199–1205.
109. Farina KL, et al. Cell motility of tumor cells visualized in living intact primary tumors using green fluorescent protein. *Cancer Res*. 1998;58(12):2528–2532.
110. Alitalo K, Tammela T, Petrova TV. Lymphangiogenesis in development and human disease. *Nature*. 2005;438(7070):946–953.
111. Meric-Bernstam F, et al. Toward nodal staging of axillary lymph node basins through intradermal administration of fluorescent imaging agents. *Biomed Opt Express*. 2014;5(1):183–196.
112. Kinmonth JB, Taylor GW, Lee RH. Arteriol replacement by orlon cloth; a preliminary report of its experimental and clinical use. *Br Med J*. 1955;1(4927):1406–1409.
113. Kos S, Haueisen H, Lachmund U, Roeren T. Lymphangiography: forgotten tool or rising star in the diagnosis and therapy of postoperative lymphatic vessel leakage. *Cardiovasc Intervent Radiol*. 2007;30(5):968–973.
114. Partsch H, Urbanek A, Wenzel-Hora B. The dermal lymphatics in lymphoedema visualized by indirect lymphography. *Br J Dermatol*. 1984;110(4):431–438.
115. Suga K, Ogasawara N, Okada M, Matsunaga N. Interstitial CT lymphography-guided localization of breast sentinel lymph node: preliminary results. *Surgery*. 2003;133(2):170–179.
116. Suga K, et al. Breast sentinel lymph node mapping at CT lymphography with iopamidol: preliminary experience. *Radiology*. 2004;230(2):543–552.
117. Kobayashi H, et al. Micro-magnetic resonance lymphangiography in mice using a novel dendrimer-based magnetic resonance imaging contrast agent. *Cancer Res*. 2003;63(2):271–276.
118. Liu NF, et al. Anatomic and functional evaluation of the lymphatics and lymph nodes in diagnosis of lymphatic circulation disorders with contrast magnetic resonance lymphangiography. *J Vasc Surg*. 2009;49(4):980–987.
119. Liu NF, Yan ZX, Wu XF. Classification of lymphatic system malformations in primary lymphoedema based on MR lymphangiography. *Eur J Vasc Endovasc Surg*. 2012;44(3):345–349.